

# Analytical Design of Permanent-Magnet Traction-Drive Motors

Chunting Chris Mi

Department of Electrical and Computer Engineering, University of Michigan, Dearborn, MI 48128 USA

**This paper presents an analytical method for the design of permanent-magnet (PM) traction-drive motors with emphasis on calculation of the magnet's volume and size. The method uses a set of formulas to properly size the magnets without the high effort of finite-element analysis (FEA). The formulas not only give optimized magnet sizes, but also provide quick solutions for the preliminary designs. The method can be used in the initial design stage to set up the base for FEA and optimization, as well as throughout the entire design and optimization process to validate a PM motor design. Numerical methods and experiments confirm the accuracy of the proposed method.**

**Index Terms**—FEA, magnet, optimization, permanent magnets (PMs), PM motors, sizing, traction drives, volume.

## I. INTRODUCTION

**P**ERMANENT-MAGNET (PM) motors have been the choices for electrical vehicle (EV) and hybrid electric vehicle (HEV) powertrain applications due to their high efficiency, compact size, high torque at low speeds, and ease of control for regenerative braking [1]. The PM motor in an HEV powertrain is operated either as a motor during normal driving or as a generator during regenerative braking and power splitting as required by the vehicle operations and control strategies. PM motors with higher power densities are also now increasingly choices for aircraft, marine, naval, and space applications.

The most commercially used PM material in traction drive motors is neodymium–ferrite–boron (Nd–Fe–B). This material has a very low Curie temperature and high temperature sensitivity. It is often necessary to increase the size of magnets to avoid demagnetization at high temperatures and high currents. On the other hand, it is advantageous to use as little PM material as possible in order to reduce the cost without sacrificing the performance of the machine.

Numerical methods, such as finite-element analysis (FEA), have been extensively used in PM motor designs, including calculating the magnet sizes [2]–[7]. However, the preliminary dimensions of an electrical machine must first be determined before one can proceed to using FEA. In addition, many commercially available computer-aided design (CAD) packages for PM motor designs, such as SPEED [8] and Rmxprt [9], require the designer to choose the sizes of magnets. The performance of the PM motor can be made satisfactory by constantly adjusting the sizes of magnets and/or repeated FEA analyses.

While sizing of magnets are one of the critical tasks of PM machine design, modern textbooks and literatures do not provide detailed procedures to the sizing of magnets in PM motors [10]–[13]. This paper presents analytical methods to calculate the volume and sizes of magnets for PM motors. The proposed methods are validated by FEA and experiments.

## II. ANALYTICAL METHOD

The equations developed by Balagurov *et al.* in [14] have been used to calculate the volume of PM material needed for PM machines. Gieras and Wing reiterated the use of such equations [15]:

$$V_m = C_V \frac{P_N}{f B_r H_c} \quad (1)$$

where  $V_m$  is the total magnet volume needed for the PM motor,  $P_N$  is the rated output power of the PM motor,  $f$  is the operation frequency,  $B_r$  is the residual magnetic flux density and  $H_c$  is the coercive force of the magnets,  $C_V$  is a coefficient in the range of 0.54 to 3.1.

Although the above formula gives a first approximation to determine the volume of magnets, it does not deal with the sizing of magnets. Besides, the formula was originally developed for ferrite and Alnico magnets, which do not possess a linear demagnetization characteristic in the second quadrant. The choice of  $C_V$  is also cumbersome or undefined.

In this paper, the formula will be derived based on a set of assumptions and then modified based on practical design considerations. The assumptions include:

- magnetic pole salience can be neglected;
- the stator resistance is negligible;
- saturation can be neglected;
- the air-gap flux is sinusoidal distributed.

Based on the above assumptions, the phasor diagram of a PM synchronous motor can be shown in Fig. 1. The input power of the PM synchronous motor can be derived from Fig. 1:

$$P_1 = mIV \cos \varphi = mIE_0 \cos \delta \quad (2)$$

where  $m$  is the number of phases,  $I$  and  $V$  are the phase voltage and phase current,  $E_0$  is the induced back electromagnetic force (EMF) per phase,  $\varphi$  is the power angle, e.g., the angle between phasor  $I$  and phasor  $V$ , and  $\delta$  is the inner power angle, e.g., the angle between phasor  $I$  and phasor  $E_0$ .

The back EMF of a PM synchronous machine with sinusoidal air-gap flux can be expressed as

$$E_0 = \sqrt{2}\pi K_w f W \Phi \quad (3)$$

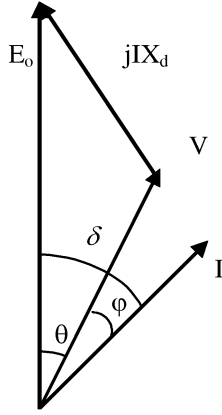


Fig. 1. Phasor diagram of PM synchronous motors.

where  $W$  is the number of turns per phase,  $\Phi$  is the total air-gap flux per pole, and  $K_w$  is the winding factor.

The phase current can be expressed in terms of armature maximum direct axis reactant magnetomotive force (MMF)  $F_{adm}$  [14]:

$$I = F_{adm} \cdot \frac{p}{0.9mWK_wK_{ad}K_m \sin \delta} \quad (4)$$

where  $K_{ad}$  is the  $d$ -axis armature reaction coefficient,  $K_m$  is the maximum possible armature current (per unit), and  $p$  is the number of poles.

Substituting (3) and (4) to (2), the input power can be expressed as

$$P_1 = \frac{\sqrt{2}\pi p f}{0.9K_{ad}K_m \tan \delta} F_{adm} \Phi. \quad (5)$$

In this paper, a new term, the magnet usage ratio  $\xi$ , is introduced and defined as follows:

$$\xi = \frac{F_{adm} \Phi_m}{F_{mo} \Phi_{mo}} \quad (6)$$

where  $\Phi_{mo}$  is the total residual flux per pole,  $F_{mo}$  is the total MMF per pole;  $\Phi_m$  is the total flux per pole at no-load condition, and  $F_{adm}$  is the maximum direct axis reactant MMF of the motor.

The definition of this magnet usage ratio is illustrated in Fig. 2, where point  $A$  is the magnet operation point at no load; and point  $B$  is the magnet operation point at maximum MMF. Air-gap flux per pole  $\Phi$  can be expressed as a function of flux supplied by the magnet  $\Phi_m$  and flux leakage coefficient  $\sigma_o$

$$\Phi = \Phi_m / \sigma_o. \quad (7)$$

For series magnets as shown in Fig. 3(a)

$$\left. \begin{aligned} \Phi_{mo} &= B_r S_m \\ F_{mo} &= 2H_c l_m \end{aligned} \right\}. \quad (8)$$

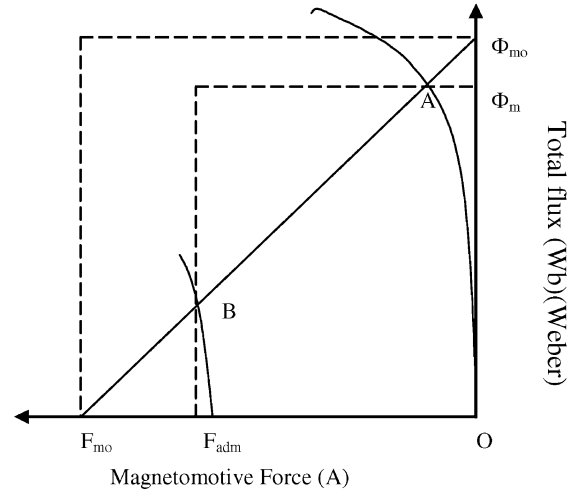
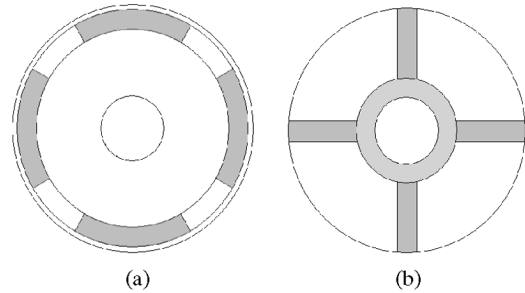
Fig. 2. Illustration of magnet usage where  $A$  is the no-load operation point and  $B$  is the maximum reversal current point.

Fig. 3. Configuration of series and parallel magnets. (a) Surface mounted with sleeve rings. (b) Parallel magnets.

For parallel magnets as shown in Fig. 3(b)

$$\left. \begin{aligned} \Phi_{mo} &= 2B_r S_m \\ F_{mo} &= H_c l_m \end{aligned} \right\} \quad (9)$$

where  $l_m$  is the thickness of magnet per pole along the magnetizing direction, and  $S_m$  is the cross section area of magnet under each pole.

Finally, the input power of the motor can be expressed as the following by substituting (6)–(9) to (5):

$$P_1 = \frac{\sqrt{2}\pi \xi f}{0.9K_{ad}K_m \sigma_o \tan \delta} B_r H_c 2p S_m l_m. \quad (10)$$

Since the total magnet volume is

$$V_m = 2p S_m l_m. \quad (11)$$

Therefore, the magnet volume used in a PM synchronous motor can be expressed as

$$V_m = \frac{0.2\sigma_o K_m K_{ad}}{\xi} \tan \delta \cdot \frac{P_1}{f B_r H_c} = C_V \frac{P_1}{f B_r H_c} \quad (12)$$

where  $C_V$  is a coefficient

$$C_V = \frac{0.2\sigma_0 K_m K_{ad}}{\xi} \tan \delta. \quad (13)$$

The equation is similar to (1). However, the coefficient calculation is more concise.

### III. PRACTICAL CONSIDERATIONS

In order to use the above equation to determine the magnet volume needed for a PM motor, certain parameters of the motor need to be identified.

#### 1. Input Power

At design stage, the input power of a PM a motor is given by

$$P_1 = \frac{P_N}{\eta \cos \varphi} \quad (14)$$

where  $\eta$  is the target efficiency and  $\cos \varphi$  is the target power factor of the motor.

#### 2. Direct Axis Armature Reaction Factor

Salience can be included in the direct axis armature reaction factor. For a given magnet coverage  $\alpha$ ,  $K_{ad}$  is [14]

$$K_{ad} = \frac{\alpha\pi + \sin \alpha\pi}{4\sin(\alpha\pi/2)}. \quad (15)$$

#### 3. Magnetic Usage Ratio and Flux Leakage Coefficient

Magnet usage ratio can be designed such that the demagnetization of magnets can be avoided. If one chooses 70%–90% residual flux and 70%–90% coercive force, then  $\zeta$  is between 0.5 and 0.81.

Flux leakage for surface-mounted magnets is usually small, e.g.,  $\sigma_o$  is approximately 1.0. For interior permanent-magnet (IPM) motors,  $\sigma_o = 1.2$ – $1.5$  and depends on the actual configuration of the motor [16].

#### 4. Maximum Armature Current

Maximum armature current happens during transient conditions, or during starting in case it is a line-start PM motor. During transient, when the PM synchronous motor runs out of synchronization, the back EMF and terminal voltage may run out of phase. Therefore, the maximum armature current always happens when the terminal voltage is out of phase with the back EMF, e.g.,

$$I_{\max} = \frac{E_o + V}{X_d} \quad (16)$$

where  $X_d$  is the direct axis reactance of the motor.

A typical value of maximum current is 4 to 8 and must be verified during the design process.

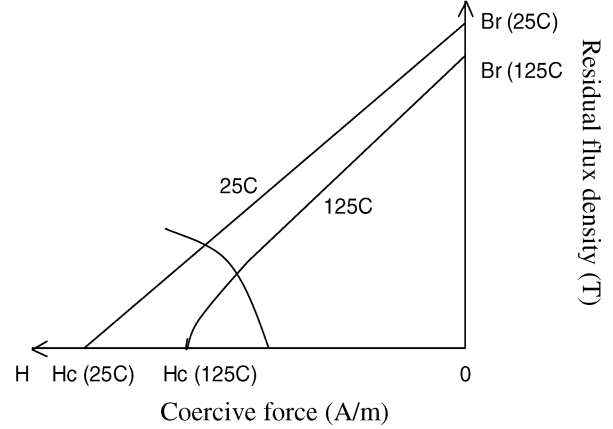


Fig. 4. Demagnetization curve considering temperature effect.

#### 5. Inner Power Angle

The power angle in (13) refers to the rated operation point. In PM motor designs, this angle is usually kept around  $25^\circ$  to  $45^\circ$ .

By substituting all the above coefficients to (12),  $C_V$  can be determined. For a reasonable first approximation,  $C_V$  can be chosen to be 2.  $C_V$  should be adjusted during the design process.

### IV. SIZING OF MAGNETS

Usually the length of magnet along the shaft direction is chosen to be the same as the rotor laminations stack length  $l_{fe}$ . The thickness of magnet along the magnetization direction is determined by the maximum armature current and operating temperature as shown in Fig. 4.

For series magnets as shown Fig. 3(a), the magnet thickness is

$$l_m = K_A \frac{K_m F_{ad}}{H_{c,125C}}. \quad (17)$$

For parallel magnets as shown in Fig. 3(b), the magnet thickness is

$$l_m = K_A \frac{K_m F_{ad}}{2H_{c,125C}} \quad (18)$$

where  $K_A$  is a safety ratio, which can be chosen to be 1.1 [8], [9], therefore

$$F_{ad} = \frac{0.9mW K_w K_{ad} \sin \delta}{p} I. \quad (19)$$

The width of rectangular magnets can be determined by

$$b_m = \frac{V_m}{2pl_m l_{fe}}. \quad (20)$$

The radius of arc-shaped magnets can be determined by

$$R = \frac{V_m}{2\pi\alpha l_m l_{fe}}. \quad (21)$$

## V. NUMERICAL METHOD

Once the initial magnet volume and sizes have been determined, FEA can be used for further design analysis and optimization. The numerical calculation will help to identify whether the volume of magnets from the preliminary design is sufficient, insufficient, or excessive. Therefore, magnet volume can be further optimized during the numerical calculations.

In PM motor design and optimization, there are many conflicting design objectives [17]–[21]. Multiobjective optimization is usually necessary in order to meet design criterion. In this paper, the optimization objective is defined as the minimal usage of PM material while satisfying the performance requirements. The optimization problem is defined as

$$\min\{V_m(X)\} \quad (22)$$

subject to

$$f_i(X) \leq 0, \quad i = 1, 2, \dots, n \quad (23)$$

where  $X$  is vector of the magnet width, thickness, and axial length

$$X = \{b_m, l_m, l_{fe}\} \quad (24)$$

$f_i(X)$  are motor performance requirements. In this paper, these requirements are defined as back EMF, efficiency, maximum torque, and short circuit current. These performances are calculated during the optimization process.

The optimization process starts with the preliminary design of the motor. The no-load magnetic field is first calculated using FEA to verify the back EMF and short circuit current. The load magnetic field is then calculated to confirm the maximum power/torque and efficiency. During each FEA, the magnet size is adjusted for given constraints.

The optimization implemented using FEA is shown in Fig. 5. Saturation, saliency, and air-gap flux waveform can also be verified during numerical calculations.

## VI. DESIGN EXAMPLES

Since most motor design CAD programs require the designer to input the preliminary design including magnet sizes, the proposed analytical method can be used to perform the preliminary design including sizing the magnets. The preliminary design can be used as input to CAD program. The design is finally optimized by using FEA.

The first design example is rated at 40 kW, 6000 rpm, four-pole, three-phase PM synchronous motor. It is designed for a parallel hybrid electric passenger vehicle.

The expected efficiency is 95% and power factor 0.95 at rated power and rated speed. To start the design,  $C_v$  is chosen to be 2.0. Using (14),  $P_1 = 44.3$  kW. Choose NdFeB material that has  $B_r = 1.26$  T,  $H_c = 0.95 \times 10^6$  A/m.  $f = 200$  Hz. Using (13), the volume of PM material can be determined to be  $V_m = 0.247 \times 10^{-3}$  m<sup>3</sup>.

During the design process, a preliminary size can be chosen based on this calculated magnet volume. It is then

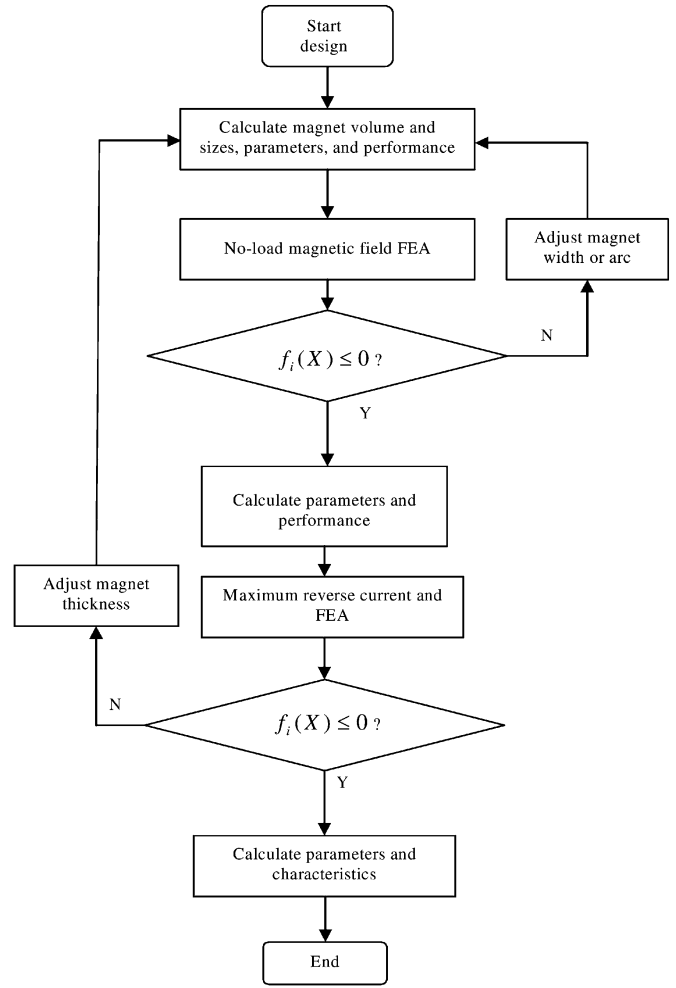


Fig. 5. Optimization of magnet usage.

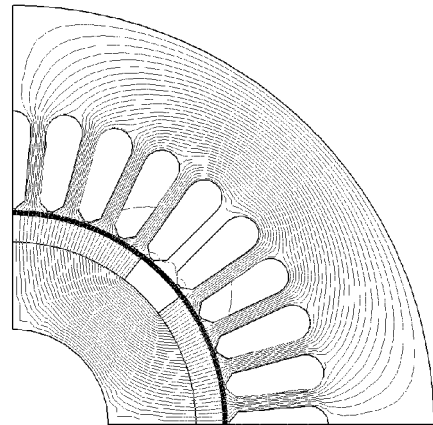


Fig. 6. Flux distribution of the 40 kW, 4-pole, 6000 rpm motor.

adjusted during the iteration of electromagnetic design. Actual  $C_v = 1.76$ . The final electromagnetic design gives  $V_m = 0.217 \times 10^{-3}$  m<sup>3</sup>.

Finally, the motor is analyzed and optimized using FEA. Fig. 6 shows the field distribution.

A second design example is a PM motor rated at 0.8 kW, 50 Hz, six-pole, three-phase PM synchronous motor, used for a small electric car. The required efficiency and power factor were

TABLE I  
MEASUREMENTS OF THE 0.8 kW PM MOTOR

EXPERIMENTS	PHASE VOLTAGE (V)	I(A)	P <sub>1</sub> (W)	P <sub>2</sub> (W)	$\eta$	PF
NO LOAD	220	0.125	54	0	0	0.655
RATED LOAD	220	1.38	880	810	92	0.966
LOCKED ROTOR	220	9.00	4740	0	0	0.798

TABLE II  
COMPARISON OF ANALYTICAL, NUMERICAL, AND MEASURED RESULTS

	PROPOSED ANALYTICAL METHOD	FEA	MEASURED
PHASE BACK EMF (V)	210.7	371	378
MAXIMUM REVERSAL CURRENT (A)	8.28	8.77	9.0
MAXIMUM REVERSAL CURRENT (PU)	6.0	6.3	6.5
FLUX LEAKAGE	1.3	1.29	1.25
POWER FACTOR	0.96	0.96	0.966
EFFICIENCY (%)	91	92.5	92

91% and 0.96, respectively, at rated power and rated speed. An induction motor frame and lamination was used to design and build the PM motor. Maximum allowed armature current was 6 p.u.

Rotor configuration of Fig. 3(b) was used. Lamination stack length was chosen to be the same as the original induction motor  $l_{fe} = 52.5$  mm. The magnet has  $B_r = 1.1$  T,  $H_c = 0.8 \times 10^6$  A/m,  $f = 50$  Hz. First approximation uses  $C_v = 2.0$ . By using equations derived in Section II, the sizes of the magnets were determined to be  $l_m = 4$  mm,  $b_m = 33$  mm. Further analysis using FEA found that  $\sigma_o = 1.29$ ,  $K_m = 6.5$ . Actual  $C_v = 2.17$ . The final electromagnetic design gives  $l_m = 4$  mm,  $b_m = 35.8$  mm. By using FEA, magnets were further optimized to be  $l_m = 4$  mm,  $b_m = 36.5$  mm.

It is worth noting that for ease of manufacturing, the magnet thickness was chosen to have increment of one half millimeter. Therefore, the final magnet thickness was not changed after optimization. However, it is shown that the final design needs 10% more magnets than it was calculated from the proposed analytical method in order to meet the efficiency and other performance requirements.

## VII. EXPERIMENTS

The 0.8 kW PM motor was built and experiments were performed. Table I shows the test results for no-load, rated load, and locked shaft test. Table II further compares the motor performance calculated using proposed analytical method, with tested results and numerical calculations. It can be seen that the experiment results matches the design very well.

## VIII. CONCLUSION

This paper proposed an improved analytical method for the design of PM traction drive motors with emphasis on deter-

mining the size and volume of permanent magnets. The FEA and experiments validated the proposed method. Although the derived formulas take the form of classical theory, it gives a more concise explanation of the coefficients used. Combined with FEA, the proposed method can provide more accurate design of magnet volume and sizes, and speed up the process of PM motor design.

The PM motor design is a rather complicated issue. General design process will involve the determination of a preliminary design, magnetic field computation using numerical method, calculation of motor parameters and performance, and optimization.

Modern numerical methods give today's engineers more powerful tools during the process of design and optimization. These methods generally require a preliminary design. Much iteration is needed before one can achieve a good design. The proposed analytical method in this paper provides a tool for the preliminary design and verification of the design during the process of iteration.

## REFERENCES

- [1] K. Muta, M. Yamazaki, and J. Tokieda, "Development of new-generation hybrid system THS II—Drastic improvement of power performance and fuel economy," presented at the SAE World Congress Detroit, MI, Mar. 8–11, 2004, SAE Paper 2004-01-0064.
- [2] S. Russenschuck, "Mathematical optimization techniques for the design of permanent magnet machines based on numerical field calculation," *IEEE Trans. Magn.*, vol. 26, no. 2, pp. 638–641, Mar. 1990.
- [3] S. Russenschuck, "Application of Lagrange multiplier estimation to the design optimization of permanent magnet synchronous machines," *IEEE Trans. Magn.*, vol. 28, no. 2, pp. 1525–1528, Mar. 1992.
- [4] K. F. Rasmussen, J. H. Davies, T. J. E. Miller, M. I. McGilp, and M. Olaru, "Analytical and numerical computation of air-gap magnetic fields in brushless motors with surface permanent magnets," *IEEE Trans. Ind. Appl.*, vol. 36, no. 6, pp. 1547–1554, Nov./Dec. 2000.
- [5] N. Boules, "Design optimization of permanent magnet DC motors," *IEEE Trans. Ind. Appl.*, vol. 26, no. 4, pp. 786–792, Jul./Aug. 1990.
- [6] A. B. Proca, A. Keyhani, A. El-Antably, W. Lu, and M. Dai, "Analytical model for permanent magnet motors with surface mounted magnets," *IEEE Trans. Energy Convers.*, vol. 18, no. 3, pp. 386–391, Sep. 2003.
- [7] D. Pavlic, V. K. Garg, J. R. Repp, and J. A. Weiss, "Finite element technique for calculating the magnet sizes and inductance of permanent magnet machines," *IEEE Trans. Energy Convers.*, vol. 3, no. 1, pp. 116–122, Mar. 1988.
- [8] T. J. E. Miller, M. McGilp, and A. Wearing, "Motor design optimization using SPEED CAD software," in *Practical Electromagnetic Design Synthesis (Ref. No. 1999/014)*, IEE Seminar, Feb. 11, 1999, pp. 2/1–2/5.
- [9] Rmxprt, Apr. 11, 2005, <http://www.ansoft.com>.
- [10] T. Kenjo and S. Nagamori, *Permanent Magnet and Brushless DC Motors*. Oxford, U.K.: Clarendon, 1985.
- [11] T. J. E. Miller, *Permanent Magnet and Reluctance Motor Drives*. Oxford, U.K.: Oxford Science Publications, 1989.
- [12] G. R. Slemon and X. Liu, "Modeling and design optimization of permanent magnet motors," *Elect. Mach. Power Syst.*, vol. 20, pp. 71–92, 1992.
- [13] B. K. Bose, *Power Electronics and Variable Frequency Drives—Technology and Applications*. Piscataway, NJ: IEEE Press, 1997.
- [14] V. A. Balagurov, F. F. Galtiev, and A. N. Laronov, *Permanent Magnet Electrical Machines* (in Russian, and translation in Chinese). Moscow, Russia: Energia, 1964.
- [15] J. F. Gieras and M. Wing, *Permanent Magnet Motor Technology: Design and Applications*, 2nd ed. New York: Marcel Dekker, 2002.
- [16] C. Mi, M. Filippa, W. Liu, and R. Ma, "Analytical method for prediction the air-gap flux of interior-type permanent magnet machines," *IEEE Trans. Magn.*, vol. 40, no. 1, pp. 50–58, Jan. 2004.
- [17] D. H. Cho, H. K. Jung, and D. J. Sim, "Multi objective optimal design of interior permanent magnet synchronous motors considering improved core loss formula," *IEEE Trans. Energy Convers.*, vol. 14, no. 4, pp. 1347–1352, Dec. 1999.

- [18] C. A. Borghi, D. Casadei, A. Cristofolini, M. Fabbri, and G. Serra, "Application of multi objective minimization technique for reducing the torque ripple in permanent magnet motors," *IEEE Trans. Magn.*, vol. 35, no. 5, pp. 4238–4246, Sep. 1999.
- [19] P. R. Upadhyay, K. R. Rajagopal, and B. P. Singh, "Effect of armature reaction on the performance of axial field permanent magnet brushless DC motor using FE method," *IEEE Trans. Magn.*, vol. 40, no. 4, pp. 2023–2025, Jul. 2004.
- [20] Y. Li, J. Zou, and Y. Lu, "Optimum design of magnet shape in permanent magnet synchronous motors," *IEEE Trans. Magn.*, vol. 39, no. 6, pp. 3523–3526, Nov. 2003.
- [21] Y. Fujishima, S. Wakao, M. Kondo, and N. Terauchi, "An optimal design of interior permanent magnet synchronous motor for the next generation commuter train," *IEEE Trans. Appl. Supercond.*, vol. 14, no. 2, pp. 1902–1905, Jun. 2004.

Manuscript received January 16, 2006 ; revised March 27, 2006. Corresponding author: C. C. Mi (e-mail: chrismi@umich.edu).

**Chunting Chris Mi** (S'00–A'01–M'01–SM'03) received the B.S.E.E. and M.S.E.E. degrees from Northwestern Polytechnical University, Xi'an, Shaanxi, China, and the Ph.D. degree from the University of Toronto, Toronto, ON, Canada, all in electrical engineering.

He is an Assistant Professor at the University of Michigan, Dearborn, with teaching and research interests in the area of power electronics, hybrid electric vehicles, electric machines and drives, renewable energy and control. He joined General Electric Canada Inc., Peterborough, ON, Canada, as an Electrical Engineer in 2000, where he was responsible for designing and developing large electric motors and generators. He was with the Rare-Earth Permanent Magnet Machine Institute of Northwestern Polytechnical University, Xi'an, Shaanxi, China, from 1988 to 1994. He joined Xi'an Petroleum Institute, Xi'an, Shaanxi, China, as an Associate Professor and Associate Chair of the Department of Automation in 1994. He was a Visiting Scientist at the University of Toronto from 1996 to 1997. He has recently developed a Power Electronics and Electrical Drives Laboratory at the University of Michigan, Dearborn.

Dr. Mi is the recipient of many technical awards, including the Government Special Allowance (China), Technical Innovation Award (China), and the Distinguished Teaching Award from the University of Michigan, Dearborn. He is the Vice Chair of the IEEE Southeastern Michigan Section.